ELSEVIER

Catalysis Today 44 (1998) 57–65

CATALYSIS TODAY

The characteristics of a copper-exchanged natural zeolite for NO reduction by NH_3 and C_3H_6

Moon Hyeon Kim, Ung-Cheon Hwang[1], In-Sik Nam*, Young Gul Kim

Department of Chemical Engineering, Research Center for Catalytic Technology, School of Environmental Engineering, Pohang University of Science and Technology (POSTECH)/Research Institute of Industrial Science and Technology (RIST), PO Box 125, Pohang 790-600, South Korea

Abstract

The catalytic performance of the natural zeolite mined from Youngil, Korea was investigated when two types of reductant such as NH_3 and hydrocarbons were employed for the reduction of NO. The determination of the structure of the natural zeolite has also been made to identify the type of zeolite and to examine its use as a catalytic material for NO removal reaction. The elementary analysis and electron probe microanalysis of the zeolite revealed that it typically consisted of an aluminosilicate. Although it mainly contains mordenite-type zeolite, heulandite was also included as well as the phases of quartz and feldspar as an impurity in the zeolite. This result could be also confirmed by the X-ray diffraction (XRD) and differential scanning calorimetry (DSC) analyses. It should be noted that the acid treatment of the natural zeolite for its use as a catalytic material is essential for the high performance of NO reduction by selective catalytic reduction (SCR) technology. Copper ion-exchanged natural zeolite catalyst (CuNZA) exhibits a competitive NO reducing activity for the reduction of NO by NH_3 as well as hydrocarbons. It can be regarded as a promising catalytic system by NH_3 and hydrocarbons for the removal of NO_x from stationary and mobile sources.

Keywords: NO reduction; Natural zeolite; Mordenite

1. Introduction

Synthetic Y-type zeolites have been widely employed for the selective catalytic reduction (SCR) of NO_x from stationary combustion sources by NH_3 [1–4]. Although copper ion-exchanged Y zeolite exhibits significant catalytic activity for the reduction of NO by NH_3, its stability is still suspicious in the acidic environment. It should be noted that flue gas streams being treated by SCR processes normally contain significant amounts of SO_x, HCl as well as NO_x.

It is well known that the acid tolerance of zeolite catalysts depends on their Si/Al ratio, and that the higher the Si/Al ratio, the higher the acid resistance. Furthermore, thermal and hydrothermal stability of zeolite catalysts also depends on their Si/Al ratio. This indicates that zeolite catalysts containing the higher Si/Al ratio may be favorable for the successful commercial application of SCR technology to actual combustion processes. Therefore, the high siliceous

*Corresponding author. Tel.: (+82-56) 279-226; fax: (+82-56) 279-8299; e-mail: isnam@postech.ac.kr

[1]Present address: System Engineering Group, Daelim Engineering Co., Yoido, PO Box 1072, Seoul 150-610, South Korea.

0920-5861/98/$32.00
PII S0920-5861(98)00173-4

zeolites such as mordenite, ferrierite, clinoptilolite and ZSM-5 may be considered as candidate catalysts for the reduction of NO_x from the flue gases.

Synthetic mordenites have been previously observed to have excellent NO_x removal activity for the selective reduction of NO by NH_3 [5–9]. Zeolite catalysts have attracted much more intensified attention, since the prominent activity of CuZSM-5 for the selective reduction of NO by hydrocarbons was revealed [10,11]. Moreover, SCR technology using hydrocarbons may be extended in its application to the reduction of NO_x contained in the exhausts of diesel and lean-burn gasoline engines. Based upon the previous studies for NO reduction by hydrocarbons [10–14], transition metal ion-exchanged zeolites, especially ZSM-5 and mordenite exhibit much higher deNO_x activity than other types of catalyst.

Naturally occurring zeolites such as mordenite, clinoptilolite and ferrierite types which contain the Si/Al ratios higher than about 5 possess high reduction efficiencies for this SCR technology by NH_3, when they contain CuO, V_2O_5 or Fe_2O_3 on their surface [15–18]. Natural zeolites including mordenite- or clinoptilolite-type were also observed to be highly active for the selective reduction of NO by hydrocarbons [19]. Not only natural zeolite mined from Youngil, Korea is not only inexpensive compared to the commercially available synthetic ones but it exhibits a competitive NO removal activity in the previous work [14,20].

In the present study, the structure of natural zeolite in the ores was determined to identify the types of zeolite present and its use as a catalytic material for NO removal reaction was examined. The catalytic performance of the natural zeolite was also tested to elucidate the characteristics of the catalyst for NO removal reaction with two types of reductant.

2. Experimental

To investigate the selective reduction of NO by NH_3 and hydrocarbons, copper ion-exchanged natural zeolite catalyst, CuNZA, was prepared from a natural zeolite mined from Youngil, Korea, as previously described elsewhere [14,20]. The natural zeolite (NZ) was treated with a 1.0 N HCl solution at 93°C for 20 h in order to remove impurities contained in the ore and to stabilize the pore structure of the zeolite. Then, CuNZA catalyst was prepared by the further treatment of NZA (NZ treated with the HCl solution) with a 1.5 N NH_4NO_3 solution followed by drying at 110°C for 10 h and calcining at 500°C for 10 h under air atmosphere and by repeatedly soaking in a 1.0 N $Cu(NO_3)_2$ solution at 93°C for 40 h. Synthetic mordenites, HM and CuHM as a reference catalyst were also prepared by similar ion-exchanging method with a Zeolon 900Na obtained from PQ corporation. The content of Cu ions in the zeolite catalysts was determined by atomic absorption spectroscopic analysis. The physicochemical properties of the prepared catalysts are listed in Table 1.

To identify the structure of the NZ employed in the present study, it was extensively examined by the catalyst characterization methods such as SEM/EPMA, differential scanning calorimetry (DSC), X-ray diffraction (XRD), FT-IR and NMR in addition to the measurement of surface area and elementary analysis. The morphology and elemental distribution of the NZ were observed by a Phillips SEM 515 instrument equipped with an Electron Probe Microanalyzer with about 5.3 eV of beam energy. X-ray powder diffraction of the NZ was measured by a M18XHF diffractometer (MAC Science) with Ni-filtered Cu K_α radiation. The FT-IR spectra for self-supporting wafers (5–10 mg/cm^2) containing the NZ were also examined at room temperature by a Perkin-Elmer 1800 Fourier transform infrared spectrophotometer with a spectral resolution of 4 cm^{-1}.

^{29}Si and ^{27}Al MAS NMR measurements for the NZ were carried out on a Bruker DPX 300 spectrometer. At the magnetic field of 7.05 T, the frequencies of ^{29}Si and ^{27}Al are 59.6 and 78.2 MHz, respectively. In the present study, a spectral width of 23.8 kHz, an acquisition time of 0.086 s, and a delay time between pulses of 2 s were used for the recording of both ^{27}Si and ^{27}Al NMR spectra. Pulse lengths of 0.01 and 0.003 ms for ^{29}Si and ^{27}Al NMR spectra, respectively, were also selected to ensure the uniform excitation of low and high electric field gradients. In addition, the NMR spectra of the synthetic mordenite (HM) as a reference were observed to compare with the structure of the NZ.

A gas composition including 500 ppm of NO, 500 ppm of NH_3 or 1000 ppm of C_3H_6 and 4.2–5.0% of O_2 was employed to observe the deNO_x efficiency of the catalysts for NO removal reaction

Table 1
Physicochemical characteristics of NZ catalysts

Catalyst	Cation content (wt%)						Si/Al	BET area (m^2/g)	Cu/Al
	Cu	Na	Ca	Fe	Mg	K			
NZ		0.86	1.99	0.76	0.63	2.37	3.87	130	
NZA		0.16	Tr	0.34	0.16	1.33	8.65	197	
NZHA							8.77		
CuNZA1	0.80								0.09
CuNZA2	1.09							203	0.12
CuNZA3	1.63	0.17	Tr	0.37	0.11	1.20	8.89	210	0.18
CuNZA4	2.90								0.32
HM							5.51	404	
CuHM1	2.20						5.10	467	0.16
CuHM2	3.54						5.02	433	0.24

in a fixed-bed flow reactor system. The reactor system and its operating condition are well described elsewhere [14,20]. For NO reduction by C_3H_6, the reactants and products were analyzed by a gas chromatography (Hewlett Packard 5890 Series II) equipped with a thermal conductivity detector. NO removal activity of the catalysts was evaluated in terms of the conversion of NO into N_2 as $2[N_2]_{out}/[NO]_{feed}$. Instead, NO removal activity for the reduction of NO by NH_3 was measured with a chemiluminescent NO–NO_x analyzer (Thermo Electron 10A) by the analysis of NO concentration in the feed and product streams of the reactor.

3. Results and discussion

3.1. Structure of NZ

3.1.1. Surface area

When the NZ was treated by HCl solution, its surface area significantly increased from 130 to 210 m^2/g as summarized in Table 1 and the mesopores ranged from 100 to 1000 Å. Its Si/Al ratio is also altered by the acid treatment with the decrease of the content of cations included in the ores of the zeolite. The addition of Cu ions to the acid-treated NZ did not change both its surface area and Si/Al ratio.

3.1.2. SEM/EPMA and chemical analysis

As shown in Fig. 1, the synthetic Na–mordenite (NaM) as a reference has well-shaped needles, which represents a well-crystallized mordenite. However, the NZ employed in this study exhibits poorly shaped needles compared to that of the synthetic mordenite. The chemical composition of the NZ corresponds to the empirical formula, $8SiO_2{\cdot}Al_2O_3{\cdot}MeO{\cdot}4H_2O$, as

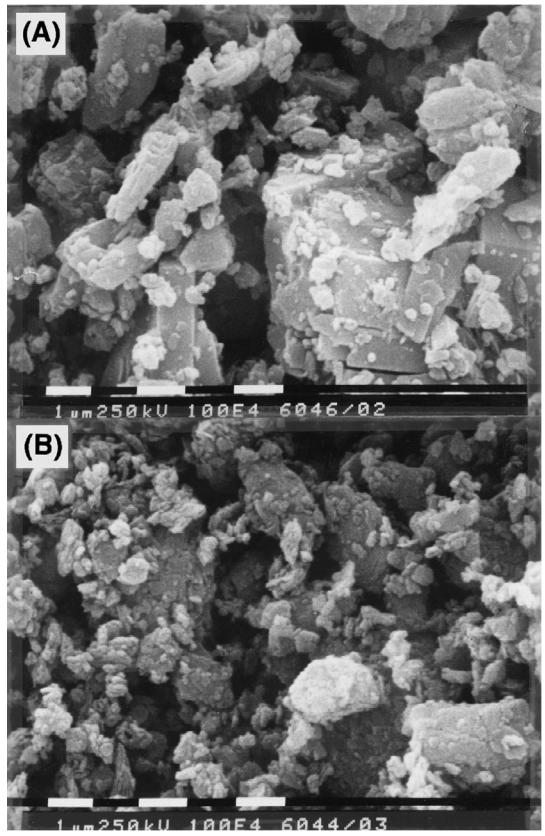

Fig. 1. Scanning electron micrographs of: (A) NaM and (B) NZ.

Table 2
Chemical analysis of the NZ employed in the present study

Oxide	Weight percent
SiO_2	67.20
Al_2O_3	14.72
CaO	2.78
K_2O	2.86
Na_2O	1.16
Fe_2O_3	1.09
MgO	1.05
RO[a]	0.16
H_2O	8.98

[a]The oxides including MnO, ZnO, NiO and BaO.

listed in Table 2. Electron probe microanalysis also indicated that major elementary compositions of the NZ are silicon and aluminum. Therefore, it is a compound which mainly consists of aluminosilicate.

A chemical formula of $10SiO_2{\cdot}Al_2O_3{\cdot}MeO{\cdot}3H_2O$ for natural clinoptilolite has been reported by Breger et al. [21]. Natural heulandite and natural mordenite exhibit chemical compositions of (6 or 7)$SiO_2{\cdot}Al_2O_3{\cdot}$ $MeO{\cdot}$(2 or 6)H_2O [21,22] and $9SiO_2{\cdot}Al_2O_3{\cdot}MeO{\cdot}$ $6H_2O$ [23], respectively. It was generally known that clinoptilolites exhibit the SiO_2/Al_2O_3 ratio of about 8.5–10.5 and the SiO_2/Al_2O_3 ratio of heulandites varies from 5.4 to 6.7 [24]. However, the NZ employed in the present study was similar to none of these chemical formulae. This is probably due to the significant amount of impurities contained in the ores of NZ.

3.1.3. *Infrared spectroscopy*

The IR absorption regions from 200 to 1300 cm^{-1} mainly reveal the fundamental vibrations of the SiO_4, AlO_4 or TO_4 units in the framework of zeolites. Therefore, they may contain useful information on the structural characteristics of the NZ employed in the present study. Fig. 2 presents the FT-IR spectra of the NZs as well as that of the synthetic mordenite (NaM and HM) as a reference. Typically, four types of absorption band at 575, 635, 725 and 805 cm^{-1} were observed for NaM. Mordenite-type zeolites are known to possess the vibration bands at the following infrared wave numbers: 448 by T–O bend, 500–650 by double ring, 650–820 by symmetric stretching and 1040–1216 cm^{-1} by asymmetric stretching [25].

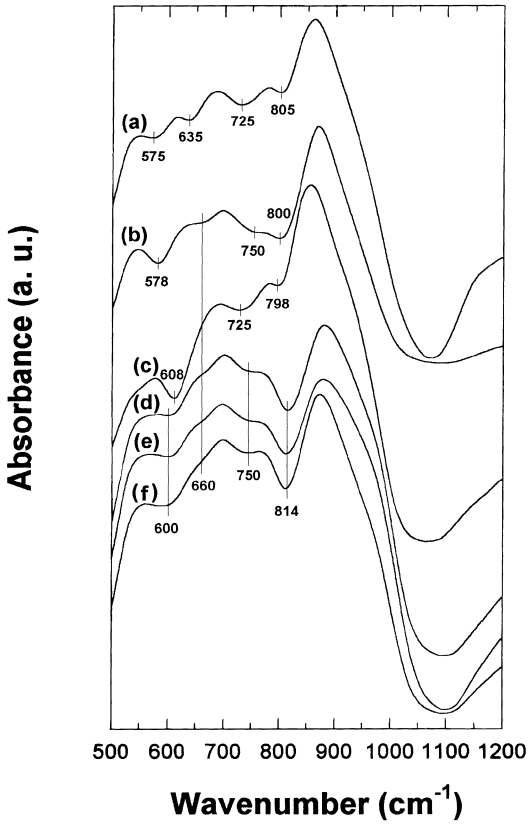

Fig. 2. IR spectra of NZ: (a) NaM, (b) HM, (c) NZ, (d) NZA, (e) NZHA and (f) CuNZA.

The NZ exhibits infrared bands at similar frequencies of 608, 725 and 798 cm^{-1}, to the synthetic mordenite. Although the absorption positions of NZ are slightly altered by the acid treatment, the IR bands of NZA, NZHA and CuNZA catalysts at 600, 660, 750 and 814 cm^{-1} are almost identical to those of HM. This suggests that the framework of the NZ is analogous to the structure of mordenite. Furthermore, it should be noted that the NZ treated with the aqueous HCl solution, NZA, shows a quite similar framework structure of the synthetic mordenite employed as a reference zeolite.

3.1.4. *Solid-state ^{27}Al and ^{29}Si MAS NMR spectroscopy*

^{27}Al MAS NMR spectra of the acid-treated NZ (NZA) and synthetic mordenite (HM) exhibited ^{27}Al peaks at about 52.5 and −2.13 ppm for both

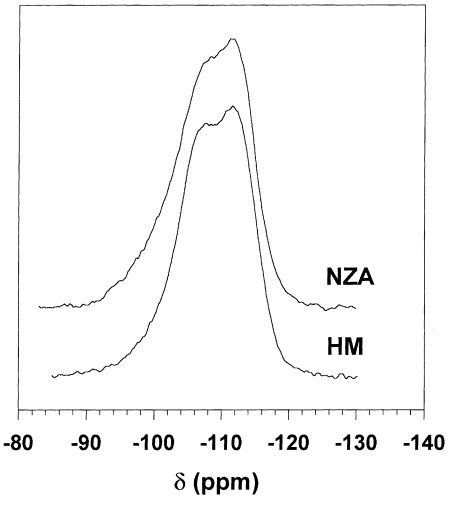

Fig. 3. ^{29}Si MAS NMR spectra of NZ and HM catalyst.

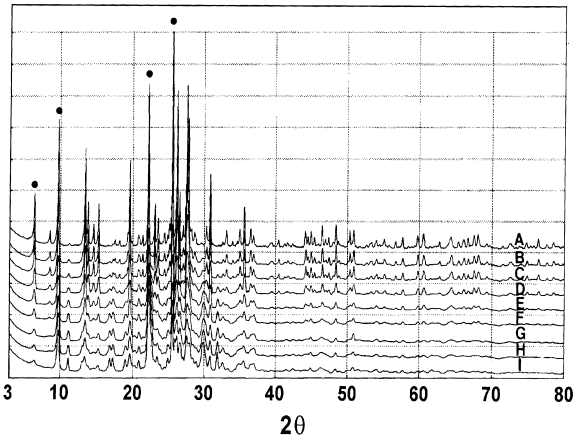

Fig. 4. XRD patterns of the physical mixtures of both synthetic mordenite and NZ. The diffractogram was recorded for: (A) 100, (B) 85, (C) 75, (D) 60, (E) 35, (F) 20, (G) 10, (H) 6 and (I) 0, where the values indicate the weight percentage of synthetic mordenite in the mixtures.

zeolites, which correspond to tetrahedrally- and octahedrally-coordinated aluminum, respectively. This reveals that the NZ contains a substantial amount of non-framework aluminum. Since aluminums in zeolites contain the environment of Al(4Si), the ^{27}Al NMR spectra of the tetrahedral lattice aluminum in their framework show only a coordination environment of aluminum in the zeolite structure. The information on the structure of the NZ can be provided from its ^{27}Si MAS NMR spectra.

Fig. 3 shows the ^{29}Si NMR spectra of NZA and HM employed in this study. The ^{29}Si spectrum of HM prepared with Zeolon 900Na (Si/Al=5.1) exhibits two intense broad peaks at −107.5 and −111.6 ppm for Si(1Al) and Si(0Al), respectively, and a very weak low-field shoulder at about −98.7 ppm for Si(2Al). This agrees well with the ^{29}Si spectra of synthetic mordenites [26,27]. Similar NMR peaks at about −107.7 and −111.4 ppm were also observed for NZA with the weak shoulder at −98.3 ppm. These three characteristic peaks indicate that the NZ employed in the present study mainly consists of mordenite-type zeolite.

3.1.5. X-ray diffraction (XRD) of NZ

The structure of the NZ was also examined by the XRD analysis against standards which are the mixtures of the NZ and synthetic mordenite. With the increase of the amount of the NZ in the mixture as shown in Fig. 4, the new peaks at 2θ=11.12, 12.96, 16.84, 17.26, 18.98, 20.30, 22.76, 23.96, 24.98, 25.96, 26.58, 28.02, 29.90, 31.88 and 32.62 were developed in addition to the unique diffraction lines of mordenite such as 2θ=6.48, 9.74, 22.20 and 25.60. The diffraction lines as mentioned above are commonly found for heulandite and clinoptilolite which exhibit identical XRD patterns at the examined diffraction angles [22,24–29]. Therefore, no distinction between heulandite and clinoptilolite can be made from the XRD analysis. An additional method is required to clarify the structure of NZ by differentiation of the characteristic peaks for their structures.

As previously observed by Mumpton [24] as well as by Sherman and Bennett [29], the prominent peaks at 2θ=26.58 and 28.02 are primarily due to the quartz and feldspar contained in the ores of NZ, respectively. Broad and diffuse peaks did not appear at the low XRD angles of 2θ=6.2 to 8.0, showing that montmorillonite was not included in the ore. The content of feldspar may be negligible among the impurities contained in the NZ as indicated in Fig. 4. It should be noted, however, that the amounts of heulandite, clinoptilolite and feldspar could not be determined because of difficulty in obtaining the pure components to use as a reference for their quantitative analysis.

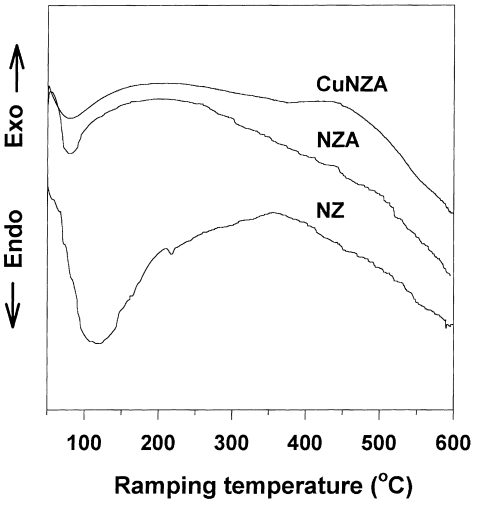

Fig. 5. DSC of NZ.

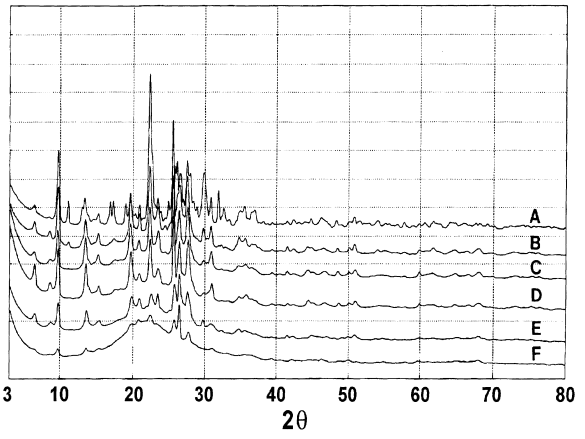

Fig. 6. XRD patterns of NZs treated with acid and high temperature treatments. The diffractogram was recorded for: (A) NZ, (B) NZ treated with a HCl solution, NZA, (C) CuNZA, (D) CuNZA heated up to 630°C, (E) CuNZA heated up to 900°C and (F) CuNZA aged at 900°C for 1 h.

3.1.6. Differential scanning calorimetry (DSC)

To identify the structures of heulandite and clinoptilolite and to obtain further information for the zeolite, the DSC profiles for the NZ and the CuNZA catalysts were examined as shown in Fig. 5. A single endothermic peak appeared at about 90–120°C, regardless of the types of zeolite catalyst examined in the present work. However, the DSC curve of the NZ significantly differs from that of the CuNZA catalyst in the temperature range from 200 to 500°C. A weak endothermic peak at about 220°C is observable for the NZ catalyst which is not treated by the acid. It is very similar to the differential thermal analyses (DTA) of natural heulandites by Mumpton [24] and Mason and Sand [30].

Although the structure of heulandite and clinoptilolite are quite similar in terms of the X-ray diffraction patterns, these two types of zeolite contain distinctive amounts of alkali metals in the zeolites. That is, the former exhibits a higher calcium content, while the latter contains more sodium and potassium in the zeolite [24]. The major difference may be the fact that heulandite undergoes a sluggish phase transition at about 230±10°C, while clinoptilolite does not [24]. It reveals that the ores of NZ include an ample amount of heulandite. It is also supported by the DSC curve for CuNZA catalyst which was prepared from NZ ores with the acid treatment (NZA).

3.1.7. XRD analysis of NZ after thermal and acid treatments

The XRD patterns of the catalysts after the thermal and acid treatments were collected to see whether clinoptilolite coexists in the NZ or not and to elucidate which of the zeolites such as mordenite, heulandite and clinoptilolite present in the NZ plays a major role for NO reduction by NH_3 and hydrocarbons. Fig. 6 shows the XRD patterns for the NZ treated with the HCl solution as well as for the CuNZA catalyst aged at high temperatures. Compared to the typical diffraction lines at 2θ=6.48, 9.74, 22.20 and 25.60 of mordenite, the peaks at 2θ=11.12, 12.96, 16.84, 17.26, 18.98, 20.30, 22.76, 23.96, 24.98, 25.96, 28.02, 29.90, 31.88 and 32.62 became weaker or were completely eliminated when the NZ was treated with the HCl solution (Fig. 6(A) and (B)). It should be noted that heulandite can be easily destroyed by acid treatment, but clinoptilolite does not significantly [24]. Therefore, the diffraction lines which disappeared may be attributed to heulandite present in the NZ. In addition, clinoptilolite may not be the major component of the NZ employed in the present study.

As shown in Fig. 6(C), CuNZA catalyst contains mainly mordenite-type zeolites. The zeolite structure of the catalyst gradually collapsed when aged at high temperatures, but the XRD peak at 2θ=26.58 is still maintained even for the catalyst aged at 900°C. It may

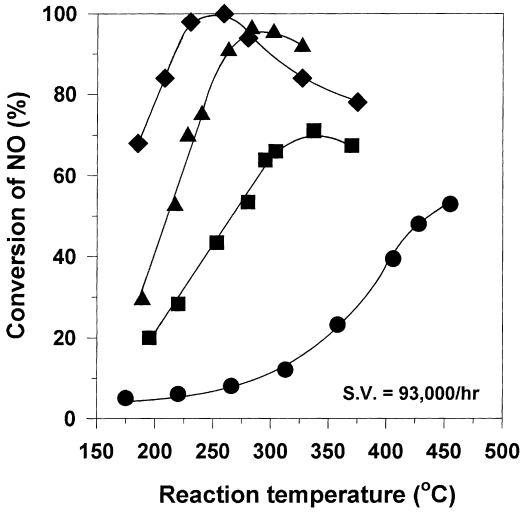

Fig. 7. $DeNO_x$ efficiency of NZ catalysts by NH_3: (●) NZA, (■) CuNZA1, (▲) CuNZA4 and (◆) CuHM1. Reaction condition: NO 500 ppm, NH_3 500 ppm and O_2 5.0%.

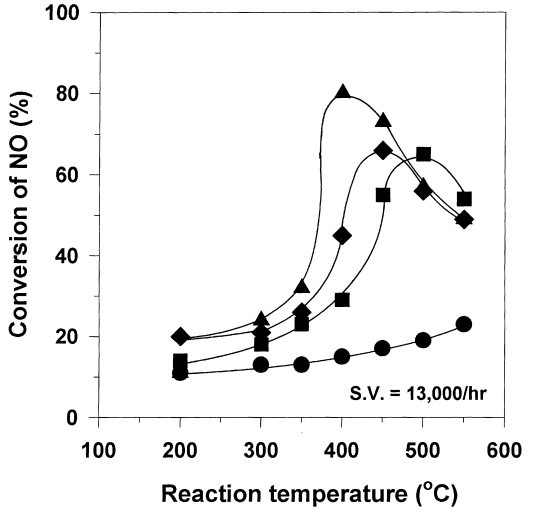

Fig. 8. $DeNO_x$ efficiency of NZ catalysts by hydrocarbons: (●) NZA, (■) CuNZA2, (▲) CuNZA3 and (◆) CuHM2. Reaction condition: NO 500 ppm, C_3H_6 1000 ppm and O_2 4.2%.

be due to the phase of a quartz thermally stable at the temperature of about 1000°C [31]. This also agrees well with the XRD result in Fig. 4.

Since CuNZA catalyst mainly contains mordenite-type zeolite, it can be expected that the catalyst will exhibit high $deNO_x$ activity with NH_3 and hydrocarbons due to the capability for ion exchange and the strong surface acidity of the catalyst. It has also been confirmed by the previous study [32].

3.2. Catalytic activity of NZ

3.2.1. SCR of NO by NH_3

Fig. 7 shows $deNO_x$ efficiency of the NZ catalyst for the selective reduction of NO by NH_3. Although the copper-free catalyst, NZA, exhibits about 50% NO conversion at the reaction temperature of 450°C, it gives less than 10% NO removal activity at reaction temperatures up to 300°C. The $deNO_x$ activity of the catalyst with NH_3 notably increases when Cu ions are introduced into the catalyst. About 95% of the conversion at 270°C was achieved for CuNZA catalyst containing 2.9 wt% of Cu ions. The net activity of the catalyst at higher reaction temperatures decreases due to a higher NH_3 oxidation rate than NO reduction rate, which is commonly observed for SCR catalysts [8,9]. The copper ions on the catalyst surface notably increase not only the NO removal activity of the zeolite catalyst but enhance NH_3 oxidation at lower reaction temperatures. CuHM catalyst as a reference shows significant NO reducing activity at reaction temperatures lower than 250°C, and the typical bell-shaped NO conversion with respect to reaction temperature is also observed as for CuNZA catalyst.

3.2.2. SCR of NO by HCs

When C_3H_6 was employed as a reductant for NO reduction, the temperature dependence of the $deNO_x$ activity of the NZ catalyst with respect to the copper content on the catalyst surface was quite similar to that for NH_3, as depicted in Fig. 8. The NZA catalyst exhibits less than about 20% NO conversion at the reaction temperatures covered in the present work, while the CuNZA catalyst shows dramatic increase of NO removal efficiency due to the introduction of Cu ions into the NZ. About 80% NO conversion for CuNZA catalyst containing 1.63 wt% of Cu ions on the catalyst surface is observed at 400°C. The copper-exchanged NZ may be a useful catalytic material for NO removal reaction compared to CuHM catalyst which exhibits about 70% NO conversion at 450°C. This indicates that the copper ions on the catalyst surface play an important role for NO reduction.

In addition, CuNZA catalyst is more active for the reduction of NO by HCs than CuHM. It may be primarily due to the higher Si/Al ratio of the catalyst. As the Si/Al ratio of zeolite increases, their surface becomes more organophillic [33]. A role of Fe and other impurities contained in the CuNZA catalyst is still under investigation.

3.2.3. *Characteristics of NZ as a SCR catalyst*

The structural analysis of the NZ by the characterizing methods such as IR, NMR, XRD and DSC reveals that it mainly consists of mordenite-type zeolite. When the copper ions were introduced into the NZ, it is very active for NO removal reaction with NH_3 as well as with hydrocarbons as a reductant. The catalytic activity can be correlated with an acidic property of the NZ. An important role of the acidity for NO reduction by NH_3 has been previously examined for synthetic mordenite catalysts, HM and CuHM [32]. The NZ also contains significant catalyst acidity as confirmed by NH_3 TPD in Fig. 9 which exhibited a similar profile to that of HM catalyst [32].

High NO removal activity of the copper ion-exchanged NZ catalyst, CuNZA was observed when C_3H_6 is employed as a reductant. The significant $deNO_x$ efficiency has also been observed for the catalytic system with C_2H_4, C_2H_6 or C_3H_8 as a reductant [14]. The amount of hydrocarbons adsorbed on the surface of CuNZA catalyst notably increased compared to that of the copper-free zeolite catalyst, NZA. It may be one of the reasons for the high $deNO_x$ performance for the reduction of NO by hydrocarbons. As previously reported for the effect of H_2O on the removal reaction, CuNZA catalyst shows a higher water tolerance than the synthetic mordenite catalysts [14]. This is primarily due to the fact that CuNZA catalyst contains a higher Si/Al ratio compared to that of the synthetic mordenites. Recently, it is also observed that the water tolerance of the CuNZA catalyst for NO reduction by hydrocarbons becomes notably stronger after dealumination of the catalyst [34].

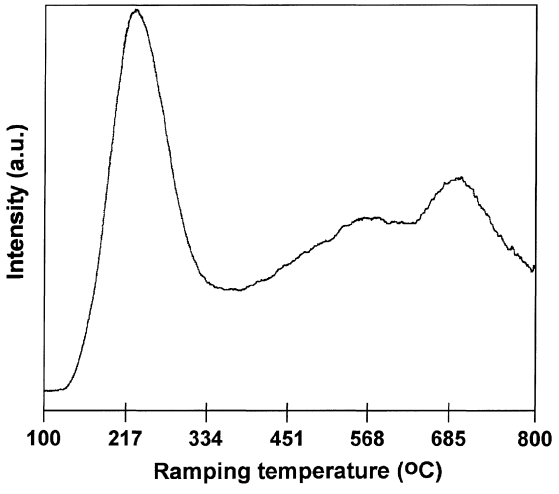

Fig. 9. NH_3 TPD profile of NZ. Temperature ramping rate was 10°C/min, and flow rate of He as a carrier gas was 40 cm^3/min.

4. Conclusions

The natural zeolite studied contains several types of zeolites such as heulandite, clinoptilolite and mordenite as well as quartz and feldspar as an impurity. Evidently, the natural zeolite treated with an acid solution mainly contains mordenite-type zeolite. It can be easily utilized as a catalytic material for SCR technology to selectively reduce NO_x. The acid treatment of the natural zeolite is essential for a higher $deNO_x$ performance. Copper ion-exchanged natural zeolite catalyst is highly active for the selective reduction of NO by NH_3 and hydrocarbons.

References

[1] H. Bosch, F. Janssen, Catal. Today 2 (1987) 369 and references therein.
[2] W.B. Williamson, J.H. Lunsford, J. Phys. Chem. 80 (1976) 2664.
[3] M. Mizumoto, N. Yamazoe, T. Seiyama, J. Catal. 55 (1978) 119.
[4] T. Seiyama, M. Mizumoto, T. Ishihara, N. Yamazoe, Ind. Eng. Chem. Prod. Res. Dev. 18 (1979) 279.
[5] J.L. Carter, M.T. Chapman, B.G. Yaokan, US Patent 3 985 094 (1975).
[6] J.R. Kiovsky, W.J. Goyette, T.M. Notermann, J. Catal. 52 (1978) 25.
[7] P.M. Hirsch, Environ. Progr. 1 (1982) 27.
[8] I.-S. Nam, J.W. Eldridge, J.R. Kittrell, Stud. Surf. Sci. Catal. 38 (1988) 589.
[9] S.-W. Ham, H. Choi, I.-S. Nam, Y.G. Kim, Catal. Today 11 (1992) 611; Ind. Eng. Chem. Res. 34 (1995) 1616.
[10] W. Held, A. Konig, T. Richter, L. Puppe, SAE Paper 900 496 (1990).

[11] M. Iwamoto, N. Mizuno, J. Auto. Eng. 207 (1993) 23 and references therein.
[12] Y. Li, J.N. Armor, Appl. Catal. B 2 (1993) 239; 3 (1993) L1; J. Catal. 145 (1994) 1.
[13] G. Mabilon, D. Durand, Catal. Today 17 (1993) 285.
[14] M.H. Kim, I.-S. Nam, Y.G. Kim, Appl. Catal. B 6 (1995) 297; 12 (1997) 125.
[15] H. Abe, S. Moriguchi, J. Takenaka, M. Miyazawa, T. Nishida, Japan Kokai, 144 371 (1976).
[16] H. Abe, J. Takenaka, Japan Kokai, 46 385 (1977).
[17] N. Fujita, C. Matsuura, T. Tamura, K. Oshima, W. Ito, N. Negishi, Nippon Kagoku Kaishi 5 (1977) 722.
[18] Y. Nishikawa, T. Maeshima, T. Itoh, S. Kamiyama, US Patent 4 104 361 (1978).
[19] T. Tamura, M. Kumagai, A. Katsuta, US Patent 5 041 272 (1991).
[20] I.-S. Nam, U.-C. Hwang, S.-W. Ham, Y.G. Kim, Proceedings of the First Tokyo Conference on Advances in Catalysis Science and Technology, Tokyo, Japan, 1990, p. 165.
[21] J.A. Breger, J.C. Chandler, P. Zubovic, Am. Mineral. 55 (1970) 825.
[22] A.B. Merkle, M. Slaughter, Am. Mineral. 53 (1968) 1120.
[23] W.T. Schaller, Am. Mineral. 17 (1932) 128.
[24] F.A. Mumpton, Am. Mineral. 45 (1960) 351.
[25] E.M. Flanigen, H. Khatami, H.A. Szymanski, Adv. Chem. Ser. 101 (1971) 201.
[26] G.R. Hays, W.V. van Erp, N.C.M. Alma, P.A. Couperus, R. Huis, A.E. Wilson, Zeolites 4 (1984) 377.
[27] P. Bodart, J.B. Nagy, G. Debras, Z. Gabelica, P.A. Jacobs, J. Phys. Chem. 90 (1986) 5183.
[28] E. Passaglia, Contrib. Mineral. Petrol. 50 (1975) 65.
[29] J.D. Sherman, J.M. Bennett, Adv. Chem. Ser. 121 (1973) 52.
[30] B. Mason, L.B. Sand, Am. Mineral. 45 (1960) 341.
[31] R.M. Barrer, M.B. Makki, Canadian J. Chem. 42 (1964) 1481.
[32] E.Y. Choi, I.-S. Nam, Y.G. Kim, J. Catal. 161 (1996) 597.
[33] K. Otto, C.N. Montreuil, O. Todor, R.W. McCabe, H.S. Gandhi, Ind. Eng. Chem. Res. 30 (1991) 2333.
[34] S.Y. Chung, M.H. Kim, I.-S. Nam, Y.G. Kim, C.B. Lee, B.S. Choi, Theor. Appl. Chem. Eng. (in Korean) 3 (1997) 3453.